Synthesis of Trimetallic Au@Pb@Pt Core-shell Nanoparticles and their Electrocatalytic Activity toward Formic Acid and Methanol

Srikanta Patra and Haesik Yang*

*Department of Chemistry and Chemistry Institute of Functional Materials, Pusan National University, Busan 609-735, Korea. *E-mail: hyang@pusan.ac.kr.*

Received January 31, 2009, Accepted May 11, 2009

A facile, seed-mediated preparation method of trimetallic Au@Pb@Pt core-shell nanoparticles is developed. Au nanoparticles are the template seeds onto which sequentially reduced Pb and Pt are deposited. The trimetallic core-shell structure is confirmed by UV-Vis spectroscopy, TEM and EDS analysis, and cyclic voltammetry. The trimetallic Au@Pb@Pt core-shell nanoparticles show high electrocatalytic activity for formic acid and methanol electrooxidation.

Key Words: Gold nanoparticle, Platinum, Lead, Electrocatalysis, Formic acid

Introduction

Metal nanoparticles have received significant attention in recent years because of their high surface-to-volume ratios and size-dependent catalytic,[1-5] optical,[6,7] and electronic properties.[8-10] When multimetallic nanoparticles are prepared in the form of an alloy or core-shell structure, their physicochemical properties can be improved in comparison to their monometallic counterparts. However, the preparation of multimetallic nanoparticles with uniform size and shape remains an active challenge in this area of research.

One-step reduction of multiple metal precursors is the easiest way to prepare multimetallic nanoparticles. However, in many cases, a large difference between standard reduction potentials of metal precursors yields a mixture of monometallic nanoparticles. Selection of suitable metal precursors having a small difference between standard reduction potentials could allow the formation of multimetallic nanoparticles.[11-13] Nevertheless, this codeposition method lacks control over size, shape, and monodispersity of multimetallic nanoparticles.[11-13] On the other hand, the seed-mediated sequential reduction method (successive deposition of one metal onto another) could allow the formation of multimetallic nanoparticles with desired sizes and shapes.[14,15]

Au nanoparticles (AuNPs) have been one of the basic seed materials for the seed-mediated preparation of multimetallic nanoparticles because of their easy preparation in various sizes and shapes.[16] In addition, their inertness to a wide range of pHs and ease of modification with other metals further makes them viable candidates for this purpose. Among the noble metals, Pt is quite attractive because of its superior catalytic activity.[17,18] A number of Pt-containing bimetallic core-shell nanoparticles such as Au@Pt,[2,4,9] Pt@Pd,[5] Pd@Pt,[19] and Pt@Ru[20,21] have been prepared, with much improved catalytic activities compared to those of pure Pt. It is also known that the combination of noble metals with Pb (such as PbPt) dramatically enhances electrocatalytic activity toward formic acid and methanol and shows a very high tolerance to CO poisoning.[11,13] Therefore, trimetallic nanoparticles consisting of AuNP seeds, Pb, and Pt could be efficient electrocatalysts for formic acid and methanol electrooxidation. To date, there is no report upon the preparation of trimetallic nanoparticles consisting of Au, Pb, and Pt.

Herein, we present a simple and efficient approach to preparing trimetallic Au@Pb@Pt core-shell nanoparticles *via* seed-mediated sequential reduction of $Pb(NO_3)_2$ and K_2PtCl_4 using $NaBH_4$ and ascorbic acid as reductants, respectively. This mild room-temperature preparation allowed the formation of monodispersed trimetallic core-shell nanoparticles. The core-shell structure of the synthesized nanoparticles was studied by cyclic voltammetry and TEM and EDS analysis. Finally, their electrocatalytic activity toward formic acid and methanol was investigated.

Experimental Section

All buffer reagents and inorganic chemicals were supplied by Sigma-Aldrich or Fluka. All chemicals were used as received. All aqueous solutions were prepared in doubly distilled water. Indium-tin oxide (ITO)-coated glass was obtained from Geomatec (Yokohama, Japan).

Citrate-stabilized AuNPs were prepared according to the Frens method.[22] Briefly, 100 mL of aqueous 0.254 mM $HAuCl_4$ was heated to a boil and 2.0 mL of 1% trisodium citrate was then added with stirring. The reaction mixture was heated for an additional 15 min and cooled to room temperature with stirring. Polyvinylpyrrolidone (1%, PVP) was then added to the solution and stirred at room temperature overnight. The final concentration of PVP in the AuNP solution was 0.1% and the average particles size of the synthesized AuNPs measured from the TEM images at 20 ± 3 nm.

Au@Pb@Pt core-shell nanoparticles were prepared by the following procedure. Deaerated aqueous $Pb(NO_3)_2$ (1.0 mL of 5.0 mM) was added to 10 mL of a deaerated aqueous solution of PVP-stabilized AuNPs, with stirring under nitrogen. After 10 min, 2.0 mL of a 50 mM $NaBH_4$ solution was added dropwise to the solution with constant stirring. The purple-colored solution turned black, indicating formation of Pb on the

AuNPs. The stirring was continued for an additional 3 h to decompose the remaining $NaBH_4$. Ascorbic acid (1.0 mL of 100 mM), followed by 1.0 mL of 20 mM K_2PtCl_4, was added with stirring and the solution stirred another 2 h at room temperature. The colloidal solution was then centrifuged twice at 20,000 g at 4 °C for 1 h and finally redispersed in 10 mL of a 0.1% PVP solution. Au@Pt core-shell nanoparticles were prepared by following the same procedure as the preparation of Au@Pb@Pt nanoparticles, except the Pb reduction step.

ITO electrodes[23] modified with amine-terminated dendrimers were prepared according to the reported procedure.[24] A colloidal solution (50 μL) was dropped and sprayed onto the dendrimer-modified ITO electrodes for 2 h, followed by washing with water, which led to the formation of nanoparticle-modified ITO electrodes.

The electrochemical experiment was performed using a CHI 708C potentiostat (CH instruments). The electrochemical cell consisted of a modified ITO working electrode, a Pt counter electrode, and an Ag/AgCl reference electrode. The area of the working electrode was 0.28 cm^2.

Results and Discussion

A schematic representation for the preparation of Au@Pb@Pt core-shell nanoparticles is shown in Scheme 1. The difference between the standard reduction potentials of Pb and Pt is quite high.[13] Pb is reduced less easily than Pt, therefore a strong reducing agent such as $NaBH_4$ is required to reduce Pb. An aqueous deaerated solution of $Pb(NO_3)_2$ was added to a deaerated PVP-stabilized AuNP solution, followed by addition of $NaBH_4$, leading to the deposition of Pb on the AuNPs. After allowing sufficient time for decomposition of the $NaBH_4$, a mild reducing agent, ascorbic acid, was added to the solution. This reducing agent was strong enough to reduce Pt^{2+} to Pt. The unstable Au@Pb nanoparticles became stable in air after the Au@Pb@Pt core-shell nanoparticles were formed. No coagulation was observed during addition of Pb $(NO_3)_2$ to the AuNP solution, as PVP was used as a stabilizer. The AuNPs acted as seeds to allow sequential deposition of Pb and Pt.

Deposition of Pb on AuNPs, followed by deposition of Pt, was visually realized by observing a distinct color change from red to black. The formation of a core-shell structure was confirmed by UV-Vis spectroscopy. Figure 1 shows the UV-Vis spectra of bare AuNPs (i in Figure 1), Au@Pb@Pt core-shell nanoparticles (ii in Figure 1), and Au@Pt core-shell nanoparticles (iii in Figure 1). The disappearance of a surface plasmon band at 520 nm, related to AuNPs upon addition of Pb (figure not shown) and Pt (ii in Figure 1), indicated the formation of Pb and Pt layers on AuNPs. Interestingly, the UV-Vis spectra of a mixed solution of the AuNPs and the Pb nanoparticles prepared *via* Pb^{2+} reduction by $NaBH_4$ (figure not shown) showed a surface plasmon band at 520 nm, indicating that the presented sequential reduction method allowed the deposition of Pb and Pt on AuNPs as a core-shell structure rather than the formation of individual monometallic nanoparticles. Similarly, in the case of Au@Pt core-shell nanoparticles, the disappearance of the surface plasmon band at 520 nm indicated the deposition of full Pt layers on AuNPs (iii in Figure 1).

Scheme 1. Schematic representation for the preparation of Au@Pb@Pt core-shell nanoparticles.

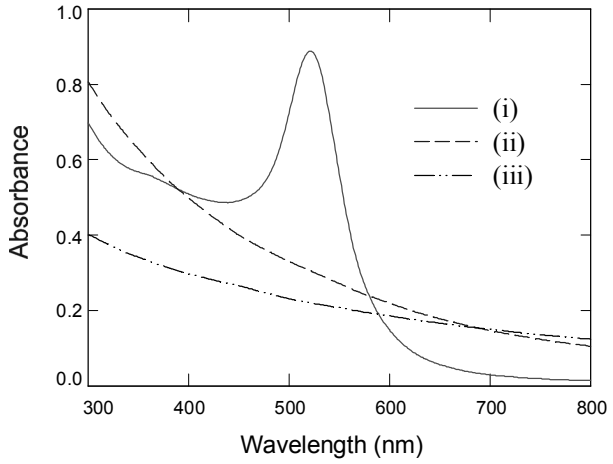

Figure 1. UV-Vis spectra of (i) AuNPs, (ii) Au@Pb@Pt nanoparticles, and (iii) Au@Pt nanoparticles recorded in aqueous 0.1% PVP. The prepared Au@Pb@Pt nanoparticle and Au@Pt nanoparticle solutions were 10-times diluted in a 0.1% PVP solution prior to measurement.

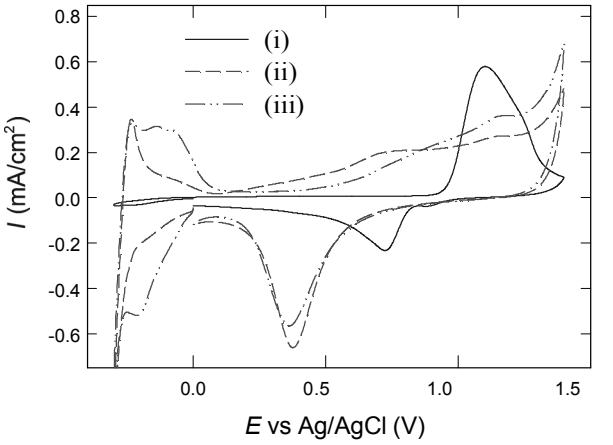

Figure 2. Cyclic voltammograms of (i) the AuNPs, (ii) the Au@Pb@Pt nanoparticles, and (iii) the Au@Pt nanoparticles on dendrimer-modified ITO electrodes recorded in a deaerated 0.1 M H_2SO_4 solution at a scan rate of 50 mV/s.

Figure 2 represents cyclic voltammograms of the AuNPs (i in Figure 2), the Au@Pb@Pt core-shell nanoparticles (ii in Figure 2), and the Au@Pt core-shell nanoparticles (iii in Figure 2) adsorbed on dendrimer-modified ITO electrodes recorded in a deaerated 0.1 M H_2SO_4 solution. The well-known hydrogen adsorption/desorption peaks related to Pt were observed

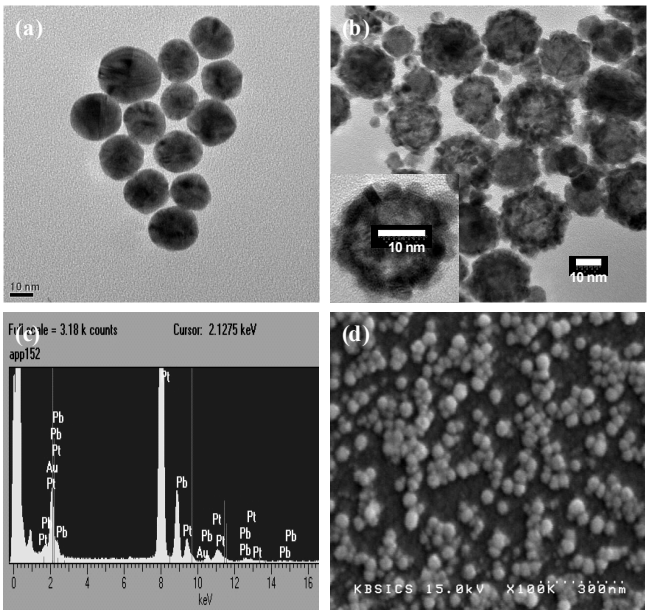

Figure 3. TEM images of (a) AuNPs and (b) Au@Pb@Pt nanoparticles, (c) EDS spectra of Au@Pb@Pt nanoparticles, and (d) SEM image of Au@Pb@Pt nanoparticles on dendrimer-modified ITO electrodes.

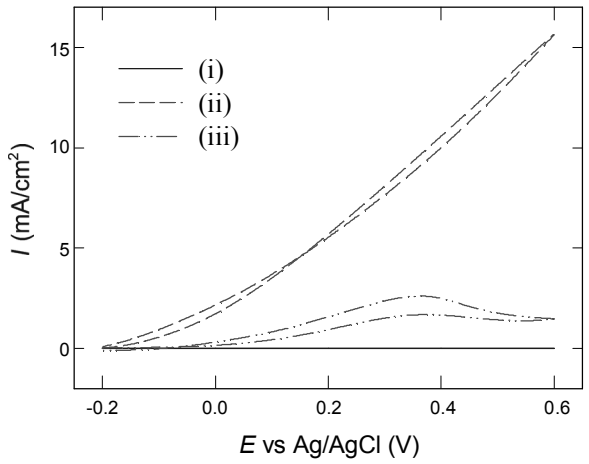

Figure 4. Cyclic voltammograms of (i) the AuNPs, (ii) the Au@Pb@Pt nanoparticles, and (iii) the Au@Pt nanoparticles on dendrimer-modified ITO electrodes obtained in 0.1 M H_2SO_4 containing 0.5 M HCOOH at a scan rate of 50 mV/s. The area in the Y-axis represents the geometric surface area of ITO electrodes.

between 0 to -0.25 V (ii and iii in Figure 2). These characteristic peaks indicated the presence of Pt on the core-shell nanoparticle-modified electrodes.[25] However, no such peaks were observed on the AuNP-modified electrodes (i in Figure 2). In addition, the peaks corresponding to the oxide formation and oxide reduction of Au at 1.1 and 0.72 V (i in Figure 2), respectively, were not observed on the Au@Pb@Pt nanoparticle-modified electrodes (ii in Figure 2) and the Au@Pt nanoparticle-modified electrodes (iii in Figure 2). This result clearly shows that the surface of Au in Au@Pb@Pt core-shell nanoparticles is fully covered with Pb and Pt layers. The appearance of a cathodic peak at 0.38 V (ii in Figure 2) related to the oxide

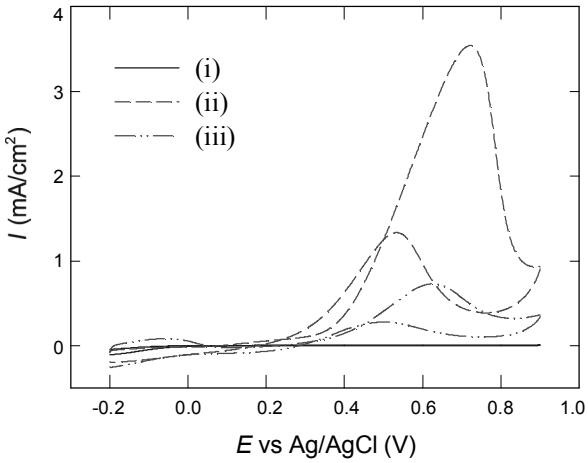

Figure 5. Cyclic voltammograms of (i) the AuNPs, (ii) the Au@Pb@Pt nanoparticles, and (iii) the Au@Pt nanoparticles on dendrimer-modified ITO electrodes obtained in 0.1 M H_2SO_4 containing 1.0 M CH_3OH at a scan rate of 50 mV/s. The area in the Y-axis represents the geometric surface area of ITO electrodes.

reduction of Pt confirms the presence of Pt.

The presence of Pb and Pt was further investigated by TEM analysis (Figure 3). Due to their instability in air, a TEM image of Au@Pb core-shell nanoparticles was not achievable. A significantly enlarged size of Au@Pb@Pt core-shell nanoparticles (28 ± 5 nm), compared to the original size of AuNPs (20 ± 3 nm) (Figure 3a) was observed after sequential reduction of Pb and Pt ions (Figure 3b), indicating the deposition of Pb and Pt onto the AuNPs. In addition, the characteristic peaks related to Au, Pb, and Pt in the EDS spectrum (Figure 3c) confirm the presence of Pb and Pt in the nanoparticles. The TEM image (Figure 3b) and SEM image (Figure 3d) show that the surface of the Au@Pb@Pt core-shell nanoparticles is rough.

It is well known that Au@Pt and PtPb nanoparticles show high electrocatalytic activity for formic acid electrooxidation.[4,5,11,13] The electrocatalytic activity of synthesized Au@Pb@Pt core-shell nanoparticles was tested and compared with that of AuNPs and Au@Pt nanoparticles in 0.1 M H_2SO_4 containing 0.5 M formic acid. Figure 4 demonstrates a comparison of electrocatalytic activities of three nanoparticles for formic acid electrooxidation. The electrocatalytic activity of Au@Pt nanoparticles (iii in Figure 4) was higher than that of AuNPs (i in Figure 4) because of the high electrocatalytic activity of Pt. The electrocatalytic activity of Au@Pb@Pt core-shell nanoparticles (ii in Figure 4) was much higher than Au@Pt nanoparticles, although the amount of Pt loading in both the Au@Pt and Au@Pb@Pt nanoparticles was almost the same (ii and iii in Figure 2 and Figure 3). This indicates that the presence of Pb in the Au@Pb@Pt nanoparticles played a crucial role in enhancing the electrocatalytic activity. Interestingly, the formic acid electrooxidation started at a very low overpotential with no significant difference between current behaviors in the forward and backward scans. These results imply that synthesized Au@Pb@Pt core-shell nanoparticles are very efficient electrocatalysts for formic acid electrooxidation and are highly tolerant of CO poisoning.[11,13]

The synthesized Au@Pb@Pt core-shell nanoparticles were also efficient in methanol electrooxidation. Figure 5 represents the cyclic voltammograms of AuNPs (i in Figure 5), Au@Pb@Pt nanoparticles (ii in Figure 5), and Au@Pt nanoparticles (iii in Figure 5) recorded in 0.1 M H_2SO_4 containing 1.0 M methanol. Expectedly, Au@Pt core-shell nanoparticles exhibited electrocatalytic activity higher than AuNPs, due to the Pt. However, Au@Pb@Pt core-shell nanoparticles showed much higher electrocatalytic activity, further confirming that the presence of Pb in Au@Pb@Pt core-shell nanoparticles significantly enhanced electrocatalytic activity.

Conclusions

We have developed a facile seed-mediated sequential reduction method for the preparation of Au@Pb@Pt core-shell nanoparticles using AuNPs as template seeds. This mild, room temperature method allowed the formation of trimetallic nanoparticles. The presence of Au, Pb, Pt, and the core-shell structure, have been confirmed by TEM and EDS analysis. The core-shell nanoparticles showed excellent electrocatalytic activity for formic acid and methanol electrooxidation. This synthetic approach could be useful to synthesize multimetallic nanoparticles with improved physicochemical properties.

Acknowledgments. This work was supported by the Nano/Bio Science & Technology Program (2005-01333) of the Ministry of Education, Science and Technology (MEST). This study was also financially supported by Pusan National University in the program, Post-Doc. 2007.

References

1. Aiken III, J. D.; Finke, R. G. *J. Mol. Catal. A* **1999**, *145*, 1.
2. Raimondi, F.; Scherer, G. G.; Kötz, R.; Wokaun, A. *Angew. Chem., Int. Ed.* **2005**, *44*, 2190.
3. Zhong, C.-J.; Maye, M. M. *Adv. Mater.* **2001**, *13*, 1507.
4. Luo, J.; Wang, L.; Mott, D.; Njoki, P. N.; Lin, Y.; He, T.; Xu, Z.; Wanjana, B. N.; Lim, I.-I. S.; Zhong, C.-J. *Adv. Mater.* **2008**, *20*, 4342.
5. Tao, F.; Grass, M. E.; Zhang, Y.; Butcher, D. R.; Renzas, J. R.; Liu, Z.; Chung, J. Y.; Mun, B. S.; Salmeron, M.; Somorjai, G. A. *Science* **2008**, *322*, 932.
6. Lima, F. H. B.; Zhang, J.; Shao, M. H.; Sasaki, K.; Vukmirovic, M. B.; Ticianelli, E. A.; Adžić, R. R. *J. Phys. Chem. C* **2007**, *111*, 404.
7. Mott, D.; Luo, J.; Njoki, P. N.; Lin, Y.; Wang, L.; Zhong, C.-J. *Catal. Today* **2007**, *122*, 378.
8. Scodeller, P.; Flexer, V.; Szamocki, R.; Calvo, E. J.; Tognalli, N.; Troiani, H.; Fainstein, A. *J. Am. Chem. Soc.* **2008**, *130*, 12690.
9. Tian, Z.-Q.; Ren, B.; Li, J.-F.; Yang, Z.-L. *Chem. Commun.* **2007**, 3514.
10. Mrozek, M. F.; Xie, Y.; Weaver, M. J. *Anal. Chem.* **2001**, *73*, 5953.
11. Matsumoto, F.; Roychowdhury, C.; DiSalvo, F. J.; Abruña, H. D. *J. Electrochem. Soc.* **2008**, *155*, B148 and references therein.
12. Wang, J.; Thomas, D. F.; Chen. A. *Anal. Chem.* **2008**, *80*, 997 and references therein.
13. Roychoudhary, C.; Matsumoto, F.; Zeldovich, V. B.; Warren, S. C.; Mutolo, P. F.; Ballesteros, M.; Wiesner, U.; Abruna, H. D.; DiSalvo, F. J. *Chem. Mater.* **2006**, *18*, 3365.
14. Toshima, N.;Yonezawa, T. *New. J. Chem.* **1998**, 1179.
15. Wang, Y.; Cai, L.; Xia, Y. *Adv. Mater.* **2005**, *17*, 473.
16. Panigrahi, S.; Basu, S.; Praharaj, S.; Pande, S.; Jana, S.; Pal, A.; Ghosh, S. K.; Pal, T. *J. Phys. Chem. C* **2007**, *111*, 4596.
17. Park, S.; Wasileski, S. A.; Weaver, M. J. *J. Phys. Chem. B* **2001**, *105*, 9719 and references therein.
18. Kunz, H. R.; Grover, G. A. *J. Electrochem. Soc.* **1975**, *122*, 1279.
19. Wang, H.; Xu, C.; Cheng, F.; Zhang, M.; Wang, S.; Jiang, S. P. *Electrochem. Commun.* **2008**, *10*, 1575.
20. Alayoglu, S.; Nilekar, A. U.; Mavrikakis, M.; Eichhorn, B. *Nature Mater.* **2008**, *7*, 333.
21. Prabhuram, J.; Zhao, T. S.; Tang, Z. K.; Chen, R.; Liang, Z. X. *J. Phys. Chem. B* **2006**, *110*, 5245.
22. Frens, G. *Nat. Phys. Sci.* **1973**, *241*, 20.
23. Aziz, M. A.; Yang, H. B. *Kor. Chem. Soc.* **2007**, *28*, 1171.
24. Das, J.; Aziz, M. A.; Yang, H. *J. Am. Chem. Soc.* **2006**, *128*, 16022.
25. Patra, S.; Das, J.; Yang, H. *Electrochim. Acta* **2009**, *54*, 3441 and references therein.